A map of cell type-specific auxin responses

Bargmann et al. Molecular Systems Biology 2013

Supplementary Information

Table of Content

Supplementary Materials and methods p2-3

Supplementary Figures p4-15

Supplementary References p16-17

Additional files:

Supplementary Table S1.xls

Expression of the auxin signaling components

Supplementary Table S2.xls

Cell type-specific auxin responses in the Arabidopsis root

Supplementary Table S3.xls

Dominant expression patterns in cell type-specific auxin responses

Supplementary Table S4.xls

Ratio's of induced-to-repressed expression of cell type-specifically enriched genes

Supplementary Table S5.xls

Analysis of publicly available microarray data

Supplementary Materials and methods

Supplementary M&m Table SM1. Plant lines used in this study.

name	description	reference
Col-0	wild type	http://www.arabidopsis.org/
DII-Venus	35S promoter driving nuclear-localized IAA28dII-Venus FP	(Vernoux et al, 2011)
DR5::3xVenus	*DR5rev* promoter driving nuclear-localized Venus FP	(Heisler et al, 2005)
pWOL::GFP	*WOODEN LEG* promoter driving ER-localized GFP in the stele	(Mahonen et al, 2000)
E3754	GAL4 enhancer-trap line marking the xylem-pole pericycle	(Gifford et al, 2008)
pWER::GFP	*WEREWOLF* promoter driving ER-localized GFP in the epidermis and lateral root cap	(Lee & Schiefelbein, 1999)
PET111	GAL4 enhancer-trap line marking the columella	(Nawy et al, 2005)
pLBD33::GUS	*LBD33* promoter driving uidA	(Okushima et al, 2007)
S6/*pATHB-8::GFP*	*ATHB-8* promoter driving ER-localized GFP	(Lee et al, 2006)
S4/*pTMO5::GFP*	*TMO5* promoter driving ER-localized GFP	(Lee et al, 2006)
S8/*pTMO6::GFP*	*TMO6* promoter driving ER-localized GFP	(Lee et al, 2006)
S18	*MYB46* promoter driving ER-localized GFP	(Lee et al, 2006)
pGH3.5::GFP	*GH3.5* promoter driving GFP	this study
pIAA5::GUS	*IAA5* promoter driving uidA	this study

Supplementary M&m Table SM2. Software and databases used in this study.

Name	Web address/reference
FlexArray 1.6.1	http://www.gqinnovationcenter.com/services/bioinformatics/flexarray/index.aspx?l=e
Q value	http://genomics.princeton.edu/storeylab/qvalue/ (Storey & Tibshirani, 2003)
Multiple Experiment Viewer	http://www.tm4.org/mev/ (Saeed et al, 2003)
Fuzzy Clustering	(Orlando et al, 2009)
VirtualPlant	http://virtualplant.bio.nyu.edu/ (Katari et al, 2010)
Raw microarray data	http://www.arexdb.org/ http://www.ncbi.nlm.nih.gov/geo/

Supplementary Figures

Supplementary Figure S1

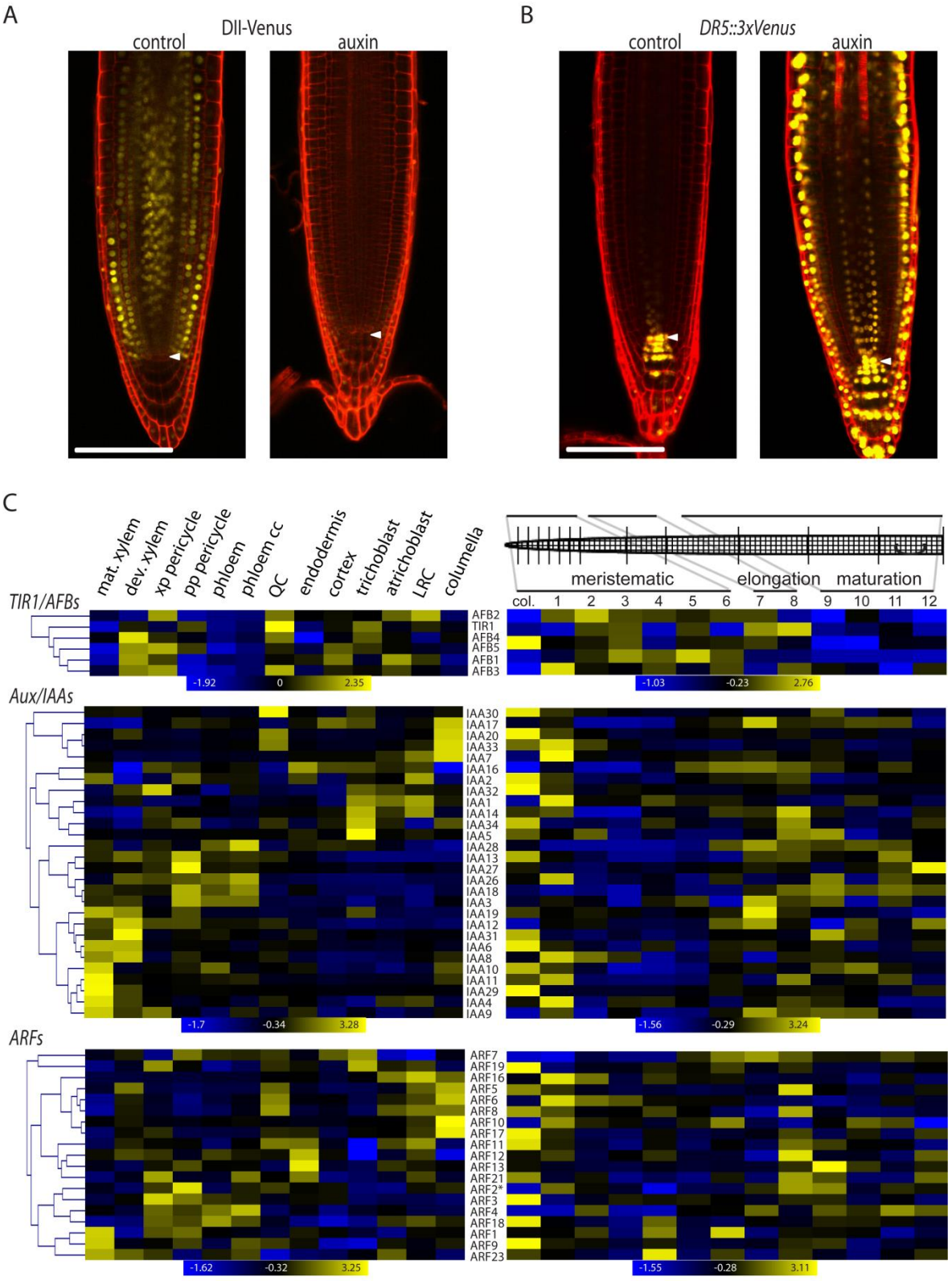

Supplementary Figure S1. Auxin-response reporters and machinery in the Arabidopsis root. A. Confocal images of the DII-Venus reporter in hydroponically grown 5 dpg seedling root tips treated with 5 µM IAA for 30 minutes (or mock treated). Cell walls were stained with propidium iodide, equal gain settings were used for YFP. Arrowheads indicate the QC, scale bar indicates 100 µm. B. Confocal images of the *DR5::3xVenus* reporter in hydroponically grown 5 dpg seedling root tips treated with 5 µM IAA for 16 h (or mock treated). Equal gain settings were used for YFP. Arrowheads indicate the QC, scale bar indicates 100 µm. C. Cell type-specific and longitudinal (root1, Brady et al, 2007) expression of the auxin response components *TIR1*/*AFBs*, *ARFs* and *Aux*/*IAAs* in select publicly available datasets of spatial expression in the Arabidopsis root (www.arexdb.org). The heatmaps consist of row-normalized gene expression with cell type and longitudinal sections of the root in columns (see Supplementary Table S1). Genes were ordered based on hierarchical clustering (Pearson correlation) of the tissue-specific dataset and visualized in the same order in the longitudinal dataset; blue (low) to yellow (high) color-code indicates standard deviations from the row mean.

Supplementary Figure S2

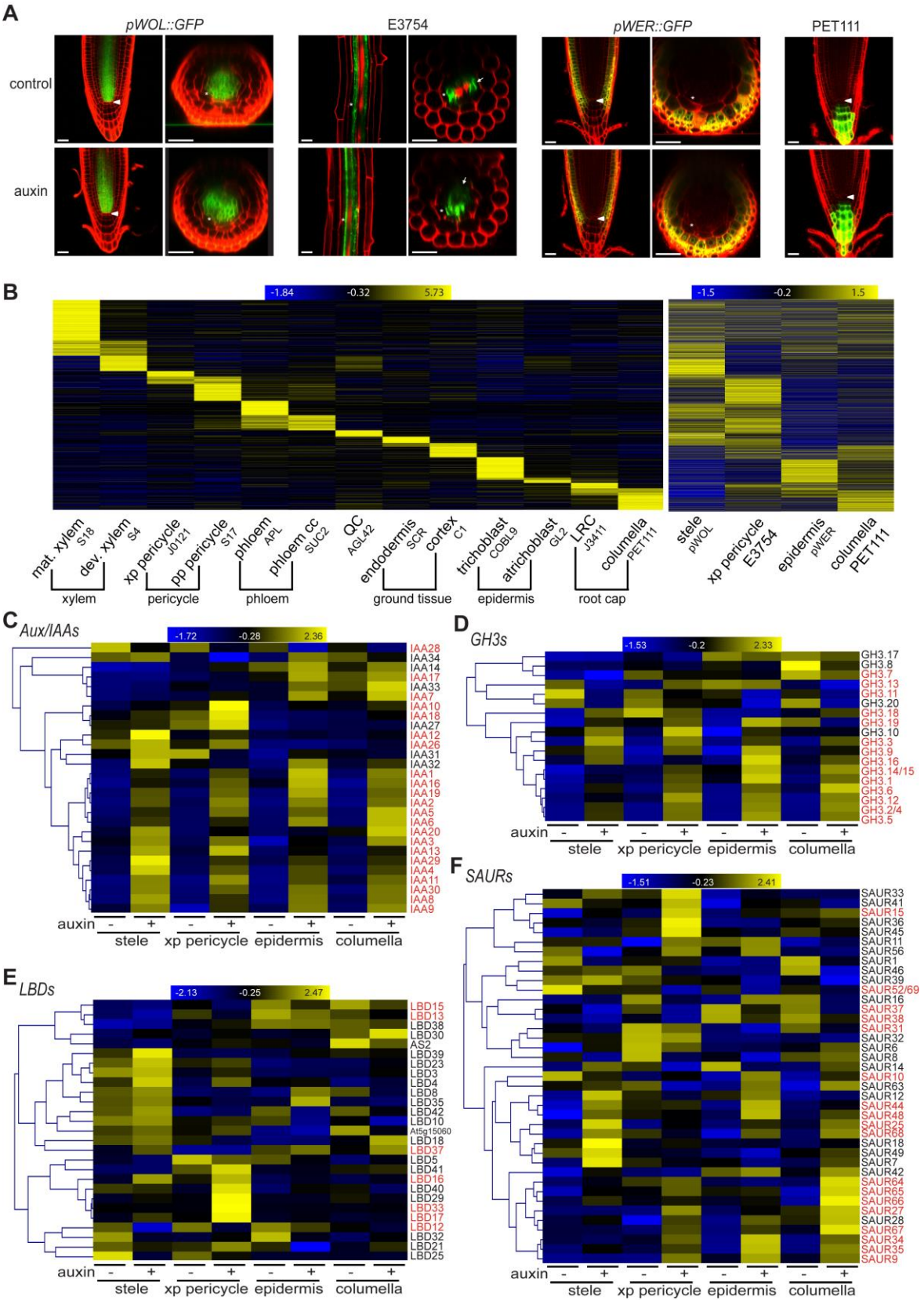

Supplementary Figure S2. Cell type-specifically enriched genes and known auxin-responsive gene families in the cell type-specific dataset. A. Micrographs of the marker lines used for cell sorting. Images were taken of control and auxin-treated roots (hydroponically grown 5 dpg seedlings treated with 5 µM IAA for 3 hours); scale bars indicate 50 µm, arrowheads indicate the QC, arrows indicate the xylem-pole and asterisks indicate the endodermis. B. 3416 genes retrieved by template matching for tissue-specific expression in 13 non-overlapping GFP marker lines (Pavlidis algorithm, R>0.8) for genes enriched in one or two closely related cell types (see Supplementary Table S2) displayed in two heatmaps of row-normalized gene expression; blue (low) to yellow (high) color-code indicates standard deviations from the row mean. The heatmap on the left shows the expression in the 13 GFP marker lines used for the template matching : S18-maturing xylem, S4-developing xylem, J0121-xp pericycle, S17-pp pericycle, APL-phloem, SUC2-phloem companion cells, AGL42-quiescent center (QC), SCR-endodermis, C1-cortex, COBL9-trichoblasts, GL2-atrichoblasts, J3411-lateral root cap (LRC), PET111-columella. The heatmap on the right shows the average expression of these genes in the 6 samples (3 mock and 3 treated) gathered for each of the four GFP markers used in this study. C-F. Spatial auxin-response patterns of known auxin-responsive gene families arranged by hierarchical clustering (pairwise Pearson correlation). Genes significantly regulated in the ANOVA for treatment or for the interaction between treatment and cell type ($p<0.01$) or passed at least one t-test for significant regulation in the four assayed tissues ($p<0.01$, fold change>1.5) are marked in red. The heatmaps consist of row-normalized gene expression with cell type +/- treatment in columns; blue (low) to yellow (high) color-code indicates standard deviations from the row mean.

Supplementary Figure S3

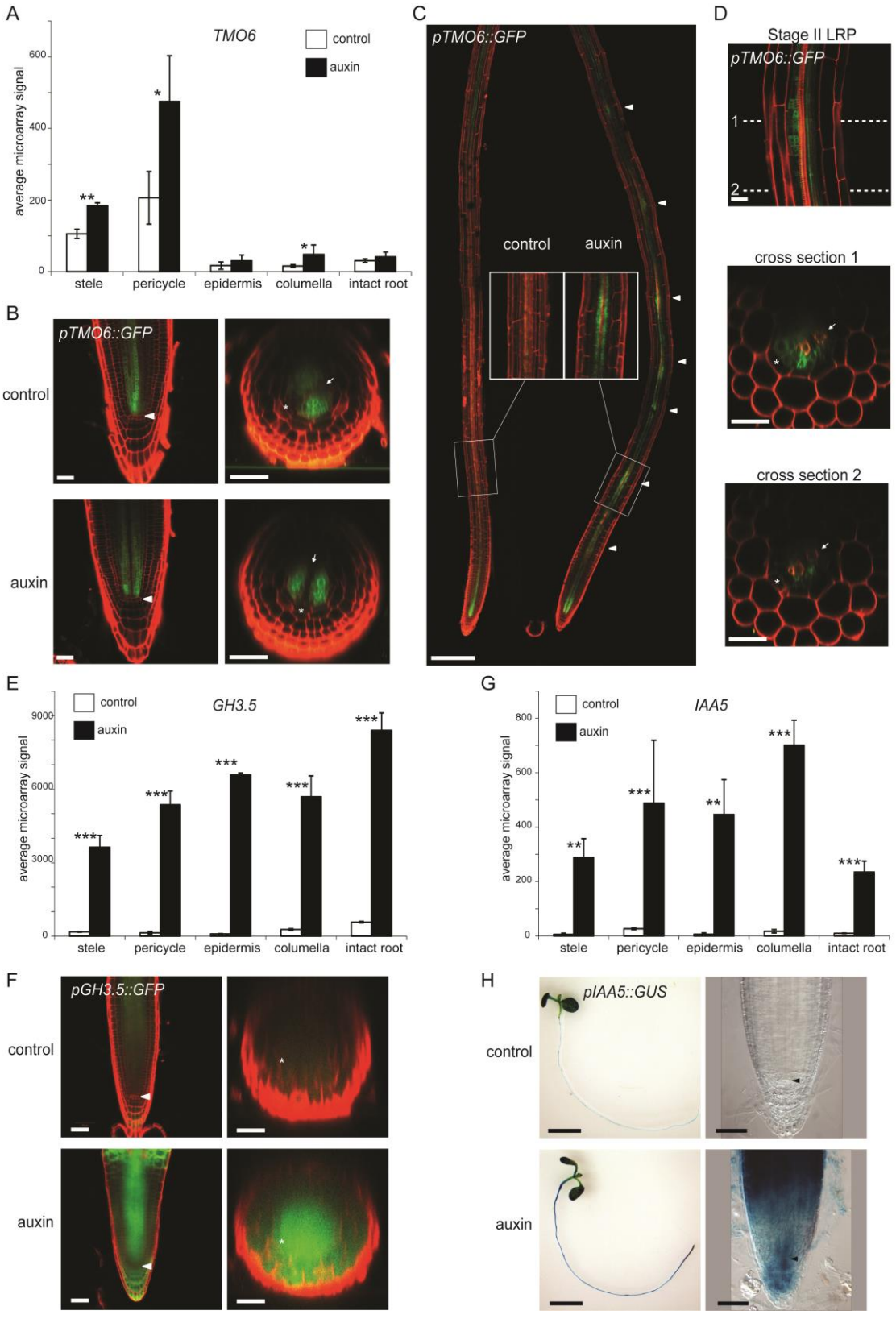

Supplementary Figure S3. Auxin-induced *TMO6, GH3.5 and IAA5* expression in the root tip. A. Histogram of microarray expression data for *TMO6*, showing induction in the xp pericycle and relatively weak induction in the stele and columella samples. Data are represented as mean +/- SD; n=3; t-test *p<0.05 **p<0.01. B-D. Confocal micrograph of *pTMO6::GFP* reporter-gene line treated with auxin (1 µM 2,4-D, 16 hours). Images were obtained with equal gain settings in the GFP channel. B. *pTMO6::GFP* expression in the root tip; scale bars indicate 25 µm, arrowheads indicate the QC, arrows indicate the xylem-pole and asterisks indicate the endodermis. C. *pTMO6::GFP* expression in auxin-induced initiating lateral roots; arrowheads indicate initiating lateral roots, scale bar indicates 250 µm. D. *pTMO6::GFP* expression in stage II lateral root primordia; dotted lines in the top panel correspond the cross-sections in the middle and lower panel, scale bars indicate 25 µm, arrows indicate the xylem-pole, asterisks indicate the endodermis. E. Histogram of microarray expression data for *GH3.5*, showing strong induction in all samples. Data are represented as mean +/-SD; n=3; t-test **p<0.01 ***p<0.001. F. Confocal micrograph of *pGH3.5::GFP* reporter-gene line treated with auxin (1 µM 2,4-D, 16 hours). Images were obtained with equal gain settings in the GFP channel; arrowhead indicates the QC, scale bars indicate 50 µm in longitudinal sections and 25 µm in radial sections. G. Histogram of microarray expression data for *IAA5*, showing strong induction in all samples. Data are represented as mean +/-SD; n=3; t-test **p<0.01 ***p<0.001. H. Micrograph of *pIAA5::GUS* reporter-gene line treated with auxin (5 µM IAA, 3 hours). Arrowhead indicates the QC, scale bars indicate 500 µm in the left panels and 50 µm in the right panels.

Supplementary Figure S4

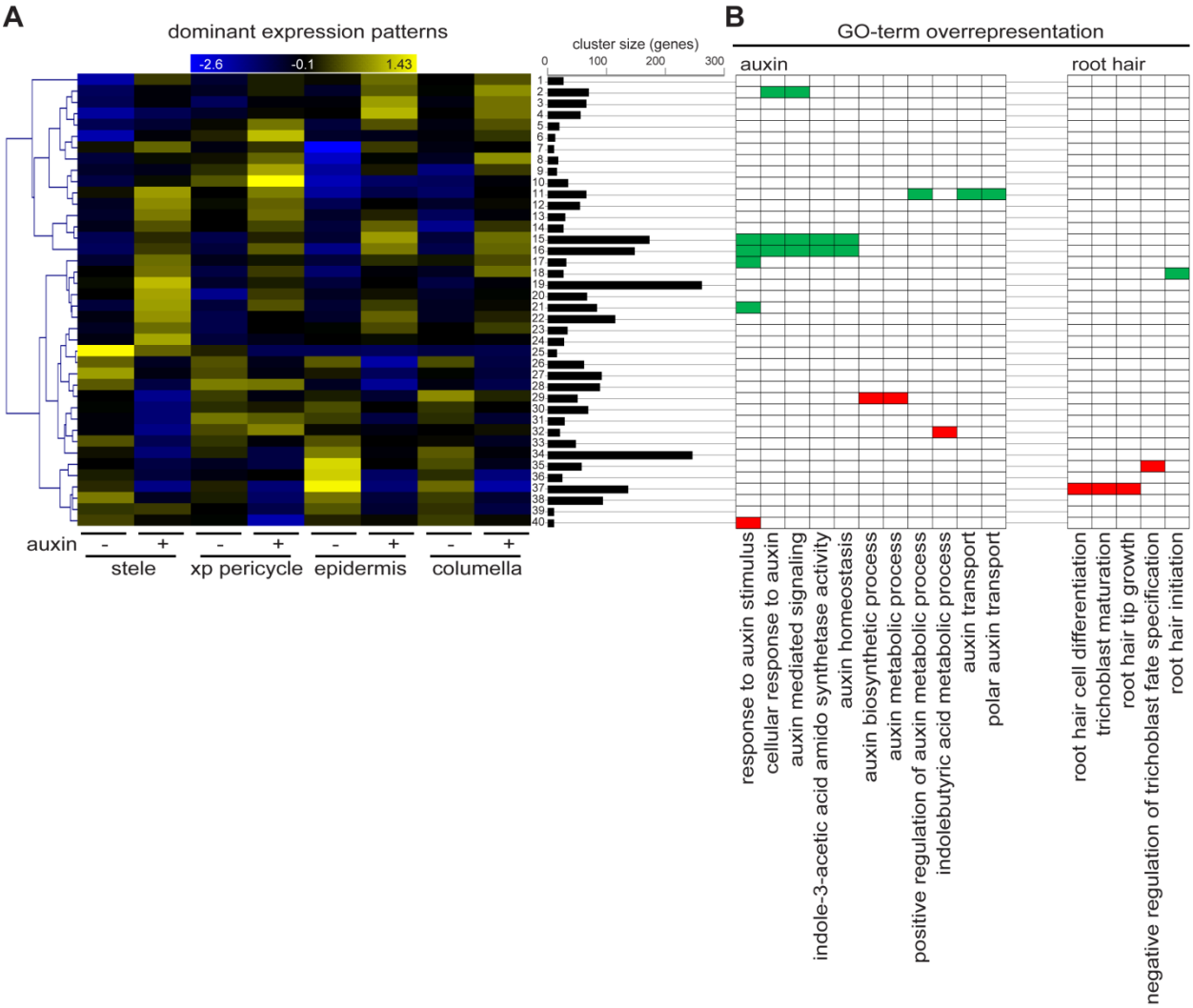

Supplementary Figure S4. Dominant expression patterns in spatial auxin responses. A. Fuzzy K-means clustering of the stringent list of 2846 auxin-responsive genes. Forty dominant expression patterns were retrieved and used to compile clusters of genes that matched these patterns. Patterns were arranged by hierarchical clustering (Pearson correlation) and are represented in a heatmap. Cluster size is indicated in a bar graph (right panel). B. Gene ontology (GO) term overrepresentation in the cluster analysis. Significantly overrepresented GO terms (corrected Fisher exact test; $p<0.01$) associated with auxin and trichoblast maturation. Up-regulated clusters are indicated in green and down-regulated clusters in red (see Supplementary Table S3).

Supplementary Figure S5

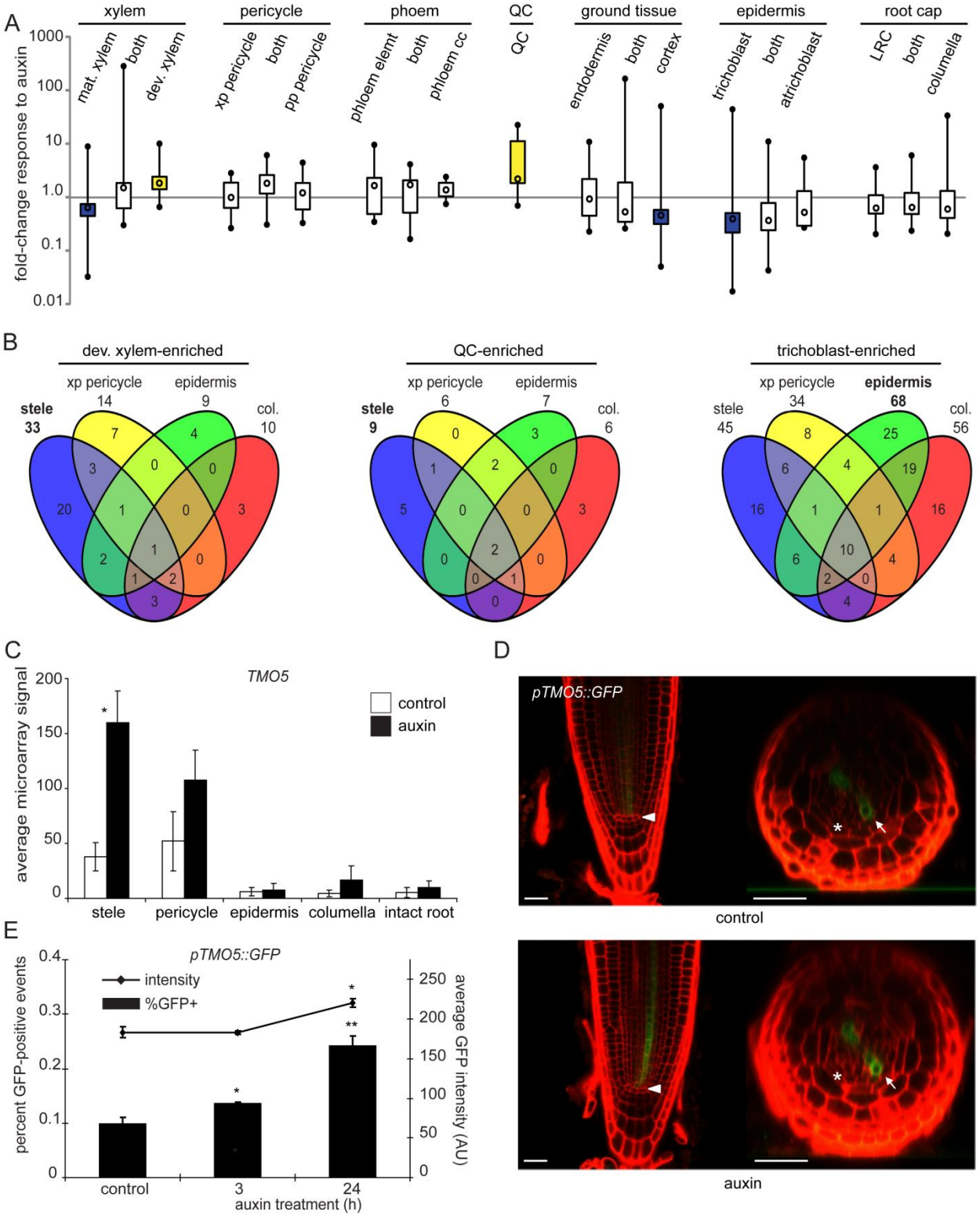

Supplementary Figure S5. Auxin affects cell type-specific transcription profiles. A. Boxplot representation of the fold-change distribution of cell-identity markers (CTSE, see Supplementary Figure S2B) that significantly respond to auxin treatment (ANOVA treatment or interaction $p<0.01$ and at least one tissue-specific t-test $p<0.01$ fold change>1.5). Black circles represent minimum and maximum values, black lines represent the first and fourth quartile, boxes represent the second and third quartile, open circle represents the median; yellow and blue coloration indicates $p<0.01$ $\chi 2$-test for ratio of induced-to-repressed genes, significantly more induced or repressed, respectively. B. Venn diagrams showing a skewed distribution of the tissue-specific t-tests ($p<0.01$ fold change>1.5) for auxin-responsive genes enriched in the developing xylem (left panel), quiescent center (middle panel) and trichoblasts (right panel). C. Histogram of microarray expression data for the *TMO5* developing-xylem identity marker, showing significant induction specifically in the stele sample. Data are represented as mean +/- SD; n=3; t-test *$p<0.01$. D. Confocal analysis of *pTMO5::GFP* reporter-gene line treated with auxin (1 µM 2,4-D, 16 h). Images were obtained with equal gain settings in the GFP channel. Arrowhead indicates the QC, arrow indicates xylem pole, asterisks indicate endodermis, scale bars indicate 25 µm. E. Cytometric quantification of the percentage of GFP-positive events and the average green fluorescent intensity of GFP-positive events in the analysis of *pTMO5::GFP* induction. Hydroponically grown seedlings were treated (5 µM IAA) and protoplasted as done for the microarray analysis (see Materials and methods). Data are represented as mean +/-SD; n=3 independent measurements; t-test *$p<0.01$, **$p<0.001$.

Supplementary Figure S6

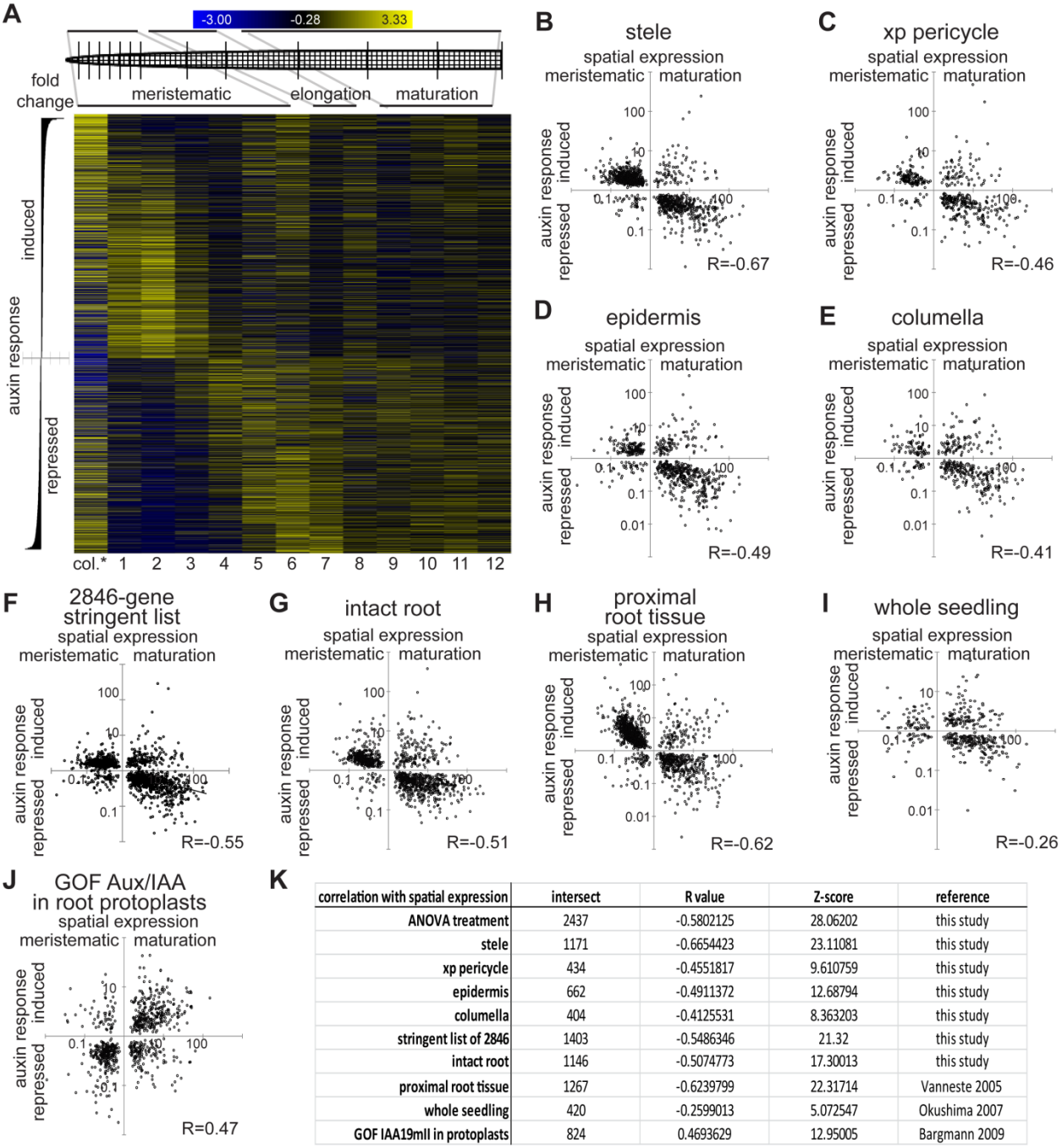

K

correlation with spatial expression	intersect	R value	Z-score	reference
ANOVA treatment	2437	-0.5802125	28.06202	this study
stele	1171	-0.6654423	23.11081	this study
xp pericycle	434	-0.4551817	9.610759	this study
epidermis	662	-0.4911372	12.68794	this study
columella	404	-0.4125531	8.363203	this study
stringent list of 2846	1403	-0.5486346	21.32	this study
intact root	1146	-0.5074773	17.30013	this study
proximal root tissue	1267	-0.6239799	22.31714	Vanneste 2005
whole seedling	420	-0.2599013	5.072547	Okushima 2007
GOF IAA19mII in protoplasts	824	0.4693629	12.95005	Bargmann 2009

Supplementary Figure S6. Independent auxin-response datasets correlate with longitudinal expression in the root. A. Heatmap of the expression of auxin-responsive genes (ANOVA treatment p<0.01, 5097 genes) in the 13-slice longitudinal dataset (root2, Brady et al, 2007). Genes were ordered by fold-change response to auxin treatment; blue (low) to yellow (high) color-code indicates standard deviations from the row mean (* there is no columella slice in the root2 dataset; the columella slice from root1 was used here). B-J. The fold-change in response to different auxin treatments (t-test p<0.01) was plotted versus the expression ratio between the meristematic zone and maturation zone (t-test p<0.01, Birnbaum et al, 2003) for the genes that are both significantly responsive to auxin and significantly differentially expressed between meristematic and maturation zones. Pearson correlation was calculated for each set. B. Auxin response in the stele (1171-gene overlap, R=-0.67). C. Auxin response in the xp pericycle (434-gene overlap, R=-0.47). D. Auxin response in the epidermis (662-gene overlap, R=-0.49). E. Auxin response in the columella (404-gene overlap, R=-0.41). F. Auxin response in the stringent list of 2846 auxin-responsive genes (1403-gene overlap, R=-0.55). G. Auxin response in the intact root (1146-gene overlap, R=-0.51). H. Auxin response in proximal root tissue (excluding the RAM; 1267-gene overlap, R=-0.62, 6 h 5 µM NAA treatment, n=2). I. Auxin response in whole seedlings (420-gene overlap, R=-0.26, 2 h 5 µM IAA treatment, n=3). J. Response to the transient over-expression of gain-of-function (GOF) *Aux*/*IAA19mII* in root protoplasts (824-gene overlap, R=0.47, n=3). K. Gene-intersect, Pearson correlation R value, Z-score for non-parametric significance test of randomized fold-change values and reference for each of the tested correlations.

Supporting References

Gifford ML, Dean A, Gutierrez RA, Coruzzi GM, Birnbaum KD (2008) Cell-specific nitrogen responses mediate developmental plasticity. *Proceedings of the National Academy of Sciences of the United States of America* **105:** 803-808

Heisler MG, Ohno C, Das P, Sieber P, Reddy GV, Long JA, Meyerowitz EM (2005) Patterns of auxin transport and gene expression during primordium development revealed by live imaging of the Arabidopsis inflorescence meristem. *Current biology : CB* **15:** 1899-1911

Katari MS, Nowicki SD, Aceituno FF, Nero D, Kelfer J, Thompson LP, Cabello JM, Davidson RS, Goldberg AP, Shasha DE, Coruzzi GM, Gutierrez RA (2010) VirtualPlant: a software platform to support systems biology research. *Plant physiology* **152:** 500-515

Lee JY, Colinas J, Wang JY, Mace D, Ohler U, Benfey PN (2006) Transcriptional and posttranscriptional regulation of transcription factor expression in Arabidopsis roots. *Proceedings of the National Academy of Sciences of the United States of America* **103:** 6055-6060

Lee MM, Schiefelbein J (1999) WEREWOLF, a MYB-related protein in Arabidopsis, is a position-dependent regulator of epidermal cell patterning. *Cell* **99:** 473-483

Mahonen AP, Bonke M, Kauppinen L, Riikonen M, Benfey PN, Helariutta Y (2000) A novel two-component hybrid molecule regulates vascular morphogenesis of the Arabidopsis root. *Genes Dev* **14:** 2938-2943

Nawy T, Lee JY, Colinas J, Wang JY, Thongrod SC, Malamy JE, Birnbaum K, Benfey PN (2005) Transcriptional profile of the *Arabidopsis* root quiescent center. *Plant Cell* **17:** 1908-1925

Okushima Y, Fukaki H, Onoda M, Theologis A, Tasaka M (2007) ARF7 and ARF19 Regulate Lateral Root Formation via Direct Activation of LBD/ASL Genes in Arabidopsis. *Plant Cell* **19:** 118-130

Orlando DA, Brady SM, Koch JD, Dinneny JR, Benfey PN (2009) Manipulating large-scale Arabidopsis microarray expression data: identifying dominant expression patterns and biological process enrichment. *Methods Mol Biol* **553:** 57-77

Saeed AI, Sharov V, White J, Li J, Liang W, Bhagabati N, Braisted J, Klapa M, Currier T, Thiagarajan M, Sturn A, Snuffin M, Rezantsev A, Popov D, Ryltsov A, Kostukovich E, Borisovsky I, Liu Z, Vinsavich A, Trush V et al (2003) TM4: a free, open-source system for microarray data management and analysis. *BioTechniques* **34:** 374-378

Storey JD, Tibshirani R (2003) Statistical significance for genomewide studies. *Proceedings of the National Academy of Sciences of the United States of America* **100:** 9440-9445

Vernoux T, Brunoud G, Farcot E, Morin V, Van den Daele H, Legrand J, Oliva M, Das P, Larrieu A, Wells D, Guedon Y, Armitage L, Picard F, Guyomarc'h S, Cellier C, Parry G, Koumproglou R, Doonan JH, Estelle M, Godin C et al (2011)

The auxin signalling network translates dynamic input into robust patterning at the shoot apex. *Molecular systems biology* **7:** 508